# Load Frequency Control of Multiarea Interconnected Power Systems With Time Delays

A. N. Gündeş and L. A. Kabuli

**Abstract**—Finite-dimensional decentralized controller design methods are developed for load-frequency control of interconnected multiarea power systems subject to time delays. Each service area may contain different types of governors and turbines, and are subject to different time delays. The controllers proposed for each service area are simple to implement, and they offer freedom in the design parameters, which may be used to improve achievable system performance. They also have integral action so that the frequency deviation outputs due to constant load disturbances go to zero asymptotically.

**Index Terms**—PID control, stable LFC design, time delay.

## I. INTRODUCTION

CONTROL of frequency and power generation is an important function of automatic generation control systems. Successful operation of a power network requires that the total generation match the total load demand and system losses. System frequency deviations due to mismatches over time cause power flows between service areas to differ from their scheduled exchanges. Load frequency control (LFC) compensates for local load changes to maintain the scheduled tie-line power flows, and achieves area control error (ACE) reduction. For a given initial operating condition, the stability of a power system is defined as its ability to regain a state of operating equilibrium after a physical disturbance occurs, with most system variables bounded so that practically the entire system remains intact [1]. The objective of power system control is to maintain stability, performance, and system integrity after failures occur, or in the presence of system disturbances, such as short circuits and loss of generation.

Power networks are important examples of networked control systems, where control loops are closed over a communication network. As in any large-scale system, time delays arising during transmission become important since time delays in LFC schemes may destabilize the closed-loop system and degrade dynamic performance. In open communication systems involving information exchange of control and feedback signals over communication networks in the form of data packages, time delays can arise during transmission from the control center to individual units and also from telemetry delays. Applications that include data networks in a control loop also introduce an network-induced delay effect in transmission between the controller and the remote system. These delays degrade the dynamic performance and may cause instability in a network-based power system.

The generation, transmission, and distribution of electric energy in modern large-scale power systems require high reliability and efficiency under uncertainty. The designs of control units and supervisory control and data-acquisition systems centers are based on rigorous robust and optimal control methodologies, infrastructure communication, and information technology services. Power systems are highly nonlinear and large-scale multi-input–multi-output dynamical systems, but a simpler linearized model can be used for the purpose of frequency control analysis and synthesis in the presence of load disturbances. Decentralized control structures offer practical advantages for large-scale multiarea frequency control synthesis since centralized controller designs are difficult to implement in a large-scale power system environment, where multiple control areas are connected through tie-lines [2]. As active power load changes, the frequencies of the service areas and tie-line power exchange deviate from scheduled values. LFC systems have been studied extensively in single-area and tie-line connected multiarea systems (see e.g., [3]–[9]) and, in some cases, with nonlinearities [10], [11]. When time delays are present in transmission, most studies consider state-space representations, while very few detailed systematic finite-dimensional controller synthesis methods have been developed, where the system is described using transfer functions [12]–[14]. Constant and time-varying delays are considered in [15], where delay margins with respect to PI gains are obtained. A delay-dependent proportional integral derivative (PID)-type analysis/synthesis method was proposed in [16], where robustness against uncertainties is guaranteed, and stability is retained for delays smaller than a preset upper bound on the delay. A PI-type decentralized LFC design based on $\mathscr{H}_\infty$ methods was proposed in [17], where it is assumed that time delays can be modeled as an unstructured multiplicative uncertainty block that contains all possible variations in the

range of delays. Robust delay-dependent PI-based LFC schemes considering the sampling-period and transmission delay based on sampled-data control were considered in [18] and [19].

This article considers the finite-dimensional stabilizing controller synthesis problem for single-area and complex tie-line interconnected multiarea power systems that are subject to time delays. For steady-state accuracy, the designed controllers here also provide integral action in order to asymptotically track step-input load disturbances with zero steady-state error, equivalently, to have zero frequency deviation in steady state due to constant loads. The designs offer freedom in the parameter selections that may improve achievable performance. When low-order stabilizing controller designs are preferred for simple implementation, the designs also include the special case of PID controllers. The proposed designs are applied to numerical studies with different types of turbines using typical values of the model parameters, as given in, e.g., [6], [12], [20], and the references therein.

The rest of this article is organized as follows. The main results are collected in Section II. The controller design for individual service areas is considered in Section II-A. A simple, straightforward design procedure is given in Proposition 1; these finite-dimensional controllers maintain closed-loop stability with integral action even in the presence of time delays. The design becomes a PID controller by selecting parameters accordingly. The controllers designed for the individual subsystems are then modified in the decentralized interconnected multiarea LFC system in Section II-B. For the multiarea closed-loop system with arbitrary time delays in each service area, the necessary and sufficient stability conditions are developed in Theorem 1 that provide results for stability analysis. The design for the individual service areas is modified in Proposition 3-a) as a decentralized integral action controller configuration that maintains closed-loop stability for prespecified time delays when the service areas are interconnected via tie-line gains. The controllers are parameterized by using a free design parameter $Q_j$ in each service area; these parameters can be varied in order to satisfy additional design specifications beyond closed-loop stability and asymptotic tracking. Proposition 3-b) treats the special case of PID controllers. Section III applies the multiarea controller design to a two-area system with a nonreheated and a reheated turbine. Finally, Section IV concludes this article.

*Notation:* Let $\mathbb{C}, \mathbb{R}$, and $\mathbb{R}_+$ denote complex, real, and positive real numbers, respectively. The closed right half-plane is $\mathbb{C}_+ = \{s \in \mathbb{C} | \Re e(s) \geq 0\}$. The region of instability is the extended closed right half-plane, i.e., $\mathbb{C}_{+e} = \mathbb{C}_+ \cup \{\infty\}$. The set of real proper rational functions of $s$ is denoted by $\mathbf{R_p}$; $\mathcal{S} \subset \mathbf{R_p}$ is the stable subset with no poles in $\mathcal{U}$. The space $\mathscr{H}_\infty$ is the set of all bounded analytic functions in $\mathbb{C}_+$. A matrix-valued function $H$ is in $\mathcal{M}(\mathscr{H}_\infty)$ if all its entries are in $\mathscr{H}_\infty$; a matrix $M \in \mathcal{M}(\mathscr{H}_\infty)$ is called unimodular if $M^{-1} \in \mathcal{M}(\mathscr{H}_\infty)$. For $f \in \mathscr{H}_\infty$, the norm $\| \cdot \|$ is defined as $\|f\| := \mathrm{ess}\sup_{s \in \mathbb{C}_+} |f(s)|$, where $\mathrm{ess}\sup$ denotes the essential supremum. Since here all norms of interest are $\mathscr{H}_\infty$ norms, the subscript is dropped, i.e., $\| \cdot \|_\infty \equiv \| \cdot \|$. When this is clear from the context, $(s)$ is dropped in transfer-functions, such as $P(s)$. We use $\mathrm{diag}[a_j]_{j=1}^k$ to denote the $(k \times k)$ diagonal matrix with entries $a_1, \ldots, a_k$.
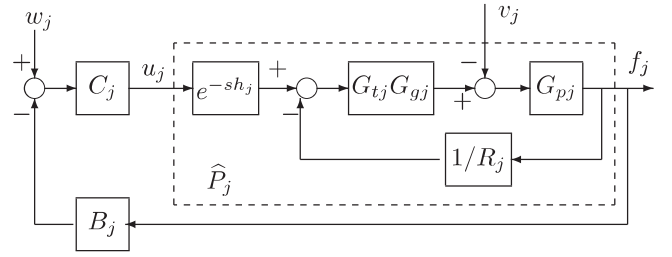


Fig. 1.    Closed-loop single-area power system $\mathscr{S}_j$.

For $W \in \mathbf{R_p}^{k \times k}$, we use coprime factorizations over $\mathscr{H}_\infty$, i.e., $W = UV^{-1}$ denotes a right-coprime-factorization of $W$, where $U, V \in \mathscr{H}_\infty^{k \times k}$, $\det V(\infty) \neq 0$.

## II. MAIN RESULTS

The LFC problem for a single generator supplying power to a single service area is considered in Section II-A. A network of multiple service areas connected by a tie-line is considered in Section II-B.

### A. Single-Area LFC With Time Delays

A linearized low-order model of the $j$th service area plant for purposes of system frequency analysis and control synthesis consists of three main parts, as shown in Fig. 1.

The transfer-functions of the load and machine, the speed governor, and the turbine are $G_{pj}(s)$, $G_{gj}(s)$, and $G_{tj}(s)$, respectively. The speed regulation due to governor action is represented by the speed droop characteristic constant $R_j$. Let $T_{pj}, T_{gj}, T_{tj}$, and $T_{rj}$ be the time-constants of the load, governor, nonreheated turbine, and reheated turbine, respectively; $K_j$ is a constant inversely proportional to the generator damping coefficient; and $c_{rj}$ is a constant for reheated turbine. The load transfer-function $G_{pj}(s)$ for all types of turbines and the governor transfer-function $G_{gj}(s)$ are given by (1). In some cases, the governors of hydraulic units include transient droop compensation for stable speed control performance [20]; in that case, $G_{gj}(s)$ for hydraulic turbines can be defined as

$$G_{pj}(s) = \frac{K_j}{T_{pj}s+1} \quad G_{gj}(s) = \frac{1}{T_{gj}s+1} \tag{1}$$

$$G_{gj}(s) = \frac{1}{(T_{gj}s+1)} \cdot \frac{(T_{cj}s+1)}{(\frac{R_{tj}}{R_j}T_{cj}s+1)}. \tag{2}$$

For nonreheated turbines, the turbine transfer-function $G_{tj}(s)$ is in (3) and for reheated turbines, it is in (4). For hydraulic turbines, the transfer-function $G_{tj}(s)$ as given in (5) contains a zero in the right-half plane at $1/T_{wj}$

$$G_{tj}(s) = \frac{1}{T_{tj}s+1} \tag{3}$$

$$G_{tj}(s) = \frac{c_{rj}T_{rj}s+1}{(T_{rj}s+1)(T_{tj}s+1)} \tag{4}$$

$$G_{tj}(s) = \frac{1-T_{wj}s}{0.5T_{wj}s+1}. \tag{5}$$

Define $X_j, Y_j$, and $P_j \in \mathcal{S}$ as follows:

$$X_j := G_{pj} G_{tj} G_{gj}, \ Y_j := 1 + R_j^{-1} X_j, \ P_j = X_j Y_j^{-1}. \quad (6)$$

For all three types of turbines (3), (4), and (5) used in generation, $X_j(0) = 1$ and $X_j(\infty) = 0$. Assuming that the speed droop characteristic $R_j$ is set for speed regulation, $Y_j^{-1}$ is stable, and, hence, $P_j$ is stable. Since $Y_j^{-1} \in \mathcal{S}$, we have $Y_j(0) = (1 + R_j^{-1} K_j) \neq 0$. Define

$$\rho_j := P_j(0) = (Y_j^{-1} G_{pj})(0) = \frac{K_j}{1 + R_j^{-1} K_j}. \quad (7)$$

With $e^{-sh_j}$ representing a delay of $h_j$ seconds, the $j$th area open-loop system $\widehat{P}_j \in \mathcal{M}(\mathscr{H}_\infty)$ is a two-input one-output plant, with $(1 \times 2)$ transfer-function from $\begin{bmatrix} u_j \\ v_j \end{bmatrix}$ to $f_j$ given by

$$\widehat{P}_j = \begin{bmatrix} P_j e^{-sh_j} & -Y_j^{-1} G_{pj} \end{bmatrix} \in \mathscr{H}_\infty^{1 \times 2}. \quad (8)$$

Now, consider the closed-loop system shown in Fig. 1. The constant $B_j \in \mathbb{R}_+$ is called the frequency bias factor for the $j$th service area. For a single-area system, the constant $B_j = 1$. This constant is used in multiarea interconnected systems in Section II-B. The input–output equations describing the $j$th area are as follows:

$$\begin{bmatrix} u_j \\ f_j \end{bmatrix} = \mathbf{H}_j \begin{bmatrix} v_j \\ w_j \end{bmatrix}$$

$$\mathbf{H}_j := (1 + e^{-sh_j} B_j P_j C_j)^{-1} \begin{bmatrix} B_j C_j G_{pj} Y_j^{-1} & C_j \\ -G_{pj} Y_j^{-1} & e^{-sh_j} P_j C_j \end{bmatrix}. \quad (9)$$

The frequency deviation map $H_j^{fv}$ from $v_j$ to $f_j$ is

$$H_j^{fv} = -(1 + e^{-sh_j} B_j X_j C_j)^{-1} G_{pj} Y_j^{-1}. \quad (10)$$

**Definition 1:**
a) The system $\mathscr{S}_j$ in Fig. 1 is stable if the closed-loop map $\mathbf{H}_j \in \mathcal{M}(\mathscr{H}_\infty)$.
b) The stable system $\mathscr{S}_j$ has integral action if the closed-loop map $\mathbf{H}_j$ is stable, and the frequency deviation transfer-function $H_j^{fv}(0) = 0$.
c) The controller $C_j$ is called a stabilizing controller for $P_j$ if $C_j$ is proper and $\mathbf{H}_j \in \mathcal{M}(\mathscr{H}_\infty)$.
d) The stabilizing $C_j$ is called an integral action controller if $C_j(s)$ has poles at $s = 0$. $\square$

Consider any coprime factorization of the controller $C_j = D_j^{-1} N_j$, where $N_j, D_j \in \mathscr{H}_\infty$, and $D_j(\infty) \neq 0$. Then, $C_j$ is a stabilizing controller if and only if $M_j^{-1} \in \mathscr{H}_\infty$, where

$$M_j := (D_j + N_j e^{-sh_j} P_j B_j). \quad (11)$$

By Definition 1-b), in the stable system $\mathscr{S}_j$, the frequency deviation output $f_j$ due to constant load disturbance $v_j$ goes to zero asymptotically if and only if it has integral action, equivalently, $H_j^{fv}(0) = 0$. Using $C_j = D_j^{-1} N_j$, write $H_j^{fv} = -(1 + e^{-sh_j} B_j P_j C_j)^{-1} G_{pj} Y_j^{-1} = -M_j^{-1} D_j G_{pj} Y_j^{-1}$. Since $G_{pj}(0) \neq 0$ and $Y_j(0) \neq 0$, by Definition 1-d), the steady-state

frequency deviation output $f_j$ due to constant load disturbance $v_j$ is zero if and only if $D_j(0) = 0$, i.e., $C_j$ is an integral action controller.

Proposition 1 presents a finite-dimensional controller design method for closed-loop stability with integral action for each individual LFC system subject to time delays. The procedure is simple, and it offers freedom in the design parameters.

***Proposition 1:*** *Design for Individual Service Areas.*
a) *General Controllers That Stabilize a Service Area:* For any $Q_j \in \mathcal{S}$, the controller $\widetilde{C}_j$ is a stabilizing controller for $P_j$, which is given by

$$\widetilde{C}_j = \frac{\beta_j Q_j}{B_j (1 - \beta_j Q_j P_j)} \quad (12)$$

where $\beta_j \in \mathbb{R}_+$ satisfies the following norm condition:

$$\beta_j < \frac{1}{h_j \|s Q_j P_j\|}. \quad (13)$$

b) *Controllers With Integral Action:* For any $Q_j \in \mathcal{S}$, an integral action controller $C_j$ is given as follows:

$$C_j = \frac{\beta_j (1 + s Q_j)}{B_j [(s + \beta_j \rho_j) - \beta_j (1 + s Q_j) P_j]} \quad (14)$$

where $\beta_j \in \mathbb{R}_+$ satisfies

$$\beta_j < \frac{1}{h_j \|(1 + s Q_j) P_j\|}. \quad (15)$$

$\square$

The controllers in Proposition 1 are parameterized by a free stable parameter $Q_j \in \mathcal{S}$, and no restrictions are imposed on the degrees of these controllers. A special case of the general controllers in (12) is a proportional+derivative (PD) controller; a special case of the integral action controllers in (14) is a PID controller. These special cases are explored in Proposition 2.

***Proposition 2:*** *PD and PID Design.*
a) *PD Controllers for Individual Service Areas:* For any $K_{pj}, K_{dj} \in \mathbb{R}$, and $\tau_j \in \mathbb{R}_+$, a special case of the controller in (12) is a PD controller as in

$$C_{\text{pd}} = \frac{\beta_j}{B_j} \left[ K_{pj} + \frac{K_{dj} s}{\tau_j s + 1} \right] \quad (16)$$

where $\beta_j$ satisfies

$$\beta_j < \left\| [K_{pj} + \frac{K_{dj} s}{\tau_j s + 1}] P_j \right\|^{-1}. \quad (17)$$

b) *PID Controllers for Individual Service Areas:* For any $K_{pj}, K_{dj} \in \mathbb{R}$, and $\tau_j \in \mathbb{R}_+$, a special case of the controller in (14) is a PID controller as in

$$C_{\text{pid}} = \frac{\beta_j}{B_j} \left[ K_{pj} + \frac{K_{dj} s}{\tau_j s + 1} + \frac{1}{s} \right] \quad (18)$$

where $\beta_j \in \mathbb{R}_+$ satisfies the following norm condition:

$$\beta_j < \left[ \| (K_{pj} + \frac{K_{dj} s}{\tau_j s + 1}) P_j + \frac{P_j - \rho_j}{s} \| \right.$$
$$\left. + h_j \| (K_{pj} s + \frac{K_{dj} s^2}{\tau_j s + 1} + 1) P_j \| \right]^{-1}. \quad (19)$$

In (16) and (18), the "derivative" term in $C_{\mathrm{pd}}$ and in $C_{\mathrm{pid}}$ is in proper (realizable) form, where $\tau_j$ is typically chosen small. $\square$

**Remarks 1:** The norm conditions (13) and (15) in Proposition 1 and the norm condition (19) in Proposition 2 determine a conservative bound on the controller parameter $\beta_j$ for a fixed time delay $h_j$. The value of $h_j$ used for these norm computations can be regarded as a guaranteed upper bound on the time delay, or the largest expected delay, but the designed controllers robustly stabilize the service area for any time delay smaller than $h_j$ as well. Due to the conservatism in the small-gain condition, the designed controller may actually result in a delay margin larger than the prespecified $h_j$ for the service area. $\square$

*Proof of Proposition 1:*

a) The controller in (12) is $\widetilde{C}_j = D_j^{-1}N_j$, with $N_j = \beta_j Q_j B_j^{-1}$ and $D_j = (1 - \beta_j Q_j P_j) = 1 - N_j B_j P_j$. Then, (11) becomes

$$M_j = (1 - \beta_j Q_j P_j) + \beta_j Q_j e^{-sh_j} B_j^{-1} B_j P_j$$

$$= 1 + \beta_j \frac{(e^{-sh_j} - 1)}{h_j s} h_j s Q_j P_j. \qquad (20)$$

For $\beta_j > 0$ satisfying (12), using the norm equality $\|(h_j s)^{-1}(e^{-sh_j} - 1)\| = 1$, it follows that

$$\left\| \beta_j \frac{(e^{-sh_j} - 1)}{h_j s} h_j s Q_j P_j \right\| \le \beta_j h_j \|s Q_j P_j\| < 1. \qquad (21)$$

Therefore, $M_j^{-1} \in \mathscr{H}_\infty$, and hence, the system $\mathscr{S}_j$ is stable with $\widetilde{C}_j$ proposed in (12).

b) The controller in (14) is $C_j = D_j^{-1}N_j$, with $N_j$ and $D_j$ as

$$N_j = \frac{\beta_j}{B_j(s + \beta_j \rho_j)}(1 + sQ_j), \quad D_j = 1 - N_j B_j P_j. \qquad (22)$$

Since $N_j(0) = \rho_j^{-1} = P_j(0)^{-1}$ implies that $D_j(0) = 0$, $C_j$ has poles at $s = 0$, i.e., $C_j$ is an integral action controller. Then, (11) becomes

$$M_j = \left(1 - \frac{\beta_j}{(s + \beta_j \rho_j)}(1 + sQ_j)P_j\right)$$

$$+ e^{-sh_j} \frac{\beta_j}{(s + \beta_j \rho_j)}(1 + sQ_j)B_j^{-1}B_j P_j$$

$$= 1 + \beta_j \frac{(e^{-sh_j} - 1)}{h_j s} \frac{h_j s}{(s + \beta_j \rho_j)}(1 + sQ_j)P_j. \qquad (23)$$

For $\beta_j > 0$ satisfying (15), using the norm equality $\|(s + \beta_j \rho_j)^{-1}s\| = 1$, it follows that

$$\left\| \beta_j \frac{(e^{-sh_j} - 1)h_j s}{h_j s(s + \beta_j \rho_j)}(1 + sQ_j)P_j \right\|$$

$$\le \beta_j h_j \|(1 + sQ_j)P_j\| < 1. \qquad (24)$$

Therefore, $M_j^{-1} \in \mathscr{H}_\infty$, and hence, the system $\mathscr{S}_j$ is stable with $C_j$ proposed in (14). $\square$

*Proof of Proposition 2:*

a) The stable controller in (16) is $C_{\mathrm{pd}} = D_j^{-1}N_j$, with $N_j = C_{\mathrm{pd}}$ and $D_j = 1$. Then, (11) becomes

$$M_j = 1 + e^{-sh_j} \frac{\beta_j}{B_j}(K_{pj} + \frac{K_{dj}s}{\tau_j s + 1})B_j P_j. \qquad (25)$$

For $\beta_j > 0$ satisfying (17), $\|e^{-sh_j} C_{\mathrm{pd}} P_j\| < 1$ implies $M_j^{-1} \in \mathscr{H}_\infty$, and hence, the system $\mathscr{S}_j$ is stable. The PD controller $C_{\mathrm{pd}}$ can be obtained from $\widetilde{C}_j$ in (12) by choosing $Q_j$ as

$$Q_j = (K_{pj} + \frac{K_{dj}s}{\tau_j s + 1})[1 + \beta_j(K_{pj} + \frac{K_{dj}s}{\tau_j s + 1})P_j]^{-1}. \qquad (26)$$

b) The controller in (16) is $C_{\mathrm{pid}} = D_j^{-1}N_j$, with $N_j$ and $D_j$ as

$$D_j = \frac{s}{(s + \beta_j \rho_j)}, \quad N_j$$

$$= \frac{\beta_j}{B_j(s + \beta_j \rho_j)}(K_{pj}s + \frac{K_{dj}s^2}{\tau_j s + 1} + 1). \qquad (27)$$

With $\beta_j > 0$ and $\rho_j > 0$, (11) becomes

$$M_j = \frac{s}{(s + \beta_j \rho_j)}$$

$$+ \frac{\beta_j}{(s + \beta_j \rho_j)}e^{-sh_j}(K_{pj}s + \frac{K_{dj}s^2}{\tau_j s + 1} + 1)P_j$$

$$= 1 + \frac{\beta_j}{(s + \beta_j \rho_j)}\left[(K_{pj}s + \frac{K_{dj}s^2}{\tau_j s + 1} + 1)P_j - \rho_j)\right.$$

$$\left. + (e^{-sh_j} - 1)(K_{pj}s + \frac{K_{dj}s^2}{\tau_j s + 1} + 1)P_j\right]$$

$$= 1 + \frac{\beta_j s}{(s + \beta_j \rho_j)}\left[(K_{pj} + \frac{K_{dj}s}{\tau_j s + 1})P_j + \frac{P_j - \rho_j}{s}\right.$$

$$\left. + \frac{(e^{-sh_j} - 1)}{sh_j}h_j(K_{pj}s + \frac{K_{dj}s^2}{\tau_j s + 1} + 1)P_j\right]. \qquad (28)$$

Using the two norm equalities: $\|s(s + \beta_j \rho_j)^{-1}\| = 1$ and $\|(h_j s)^{-1}(e^{-sh_j} - 1)\| = 1$, for $\beta_j$ satisfying the norm condition (19), it follows that $M_j^{-1} \in \mathscr{H}_\infty$, and hence, the system $\mathscr{S}_j$ is stable with the controller $C_{\mathrm{pid}} \in \mathbf{R_p}$ in (18). By Definition 1-d), $C_{\mathrm{pid}}$ is an integral action controller since it has a pole at $s = 0$. $\square$

## B. Multiarea Interconnected LFC System With Time Delays

In a large-scale interconnected power system, multiple areas are connected via tie-lines. When the frequencies in individual areas are different, a power exchange occurs through the tie-line that connects these areas. The multiarea interconnected system is shown in Fig. 2 , where each area has the same structure as the one shown in detail. The individual areas may have either one of the governor transfer-functions given in (1) or (2), and any of the turbines given in (3)–(5).
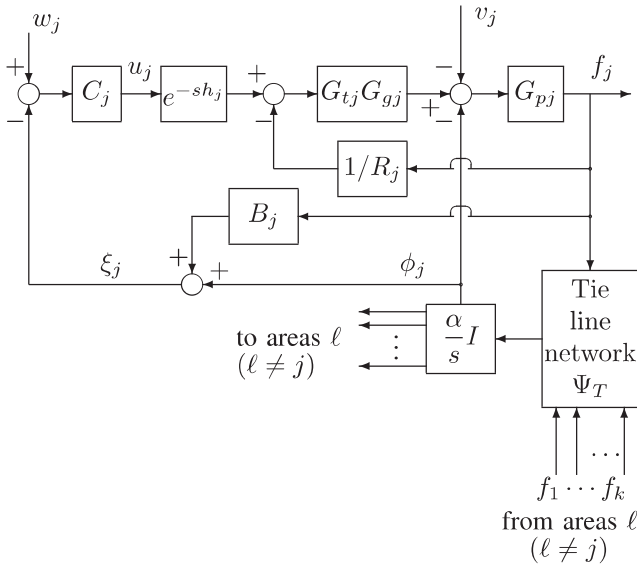
**Fig. 2.** Multiarea system $\mathscr{S}^k$; area $j$ is shown in detail.

In Fig. 2, with the constant $B_j$ denoting the frequency bias factor for the $j$th service area, the ACE signal $\xi_j$ used in feedback is

$$\xi_j = \phi_j + B_j f_j. \tag{29}$$

Define the input vectors $v$ and $w$, and the output vectors $u$, $f$, and $\xi$ as follows:

$$v = \begin{bmatrix} v_1 \\ \vdots \\ v_k \end{bmatrix}, w = \begin{bmatrix} w_1 \\ \vdots \\ w_k \end{bmatrix}, u = \begin{bmatrix} u_1 \\ \vdots \\ u_k \end{bmatrix}, f = \begin{bmatrix} f_1 \\ \vdots \\ f_k \end{bmatrix}, \xi = \begin{bmatrix} \xi_1 \\ \vdots \\ \xi_k \end{bmatrix}.$$

With $X_j = G_{pj}G_{tj}G_{gj}$ as given in (6), define the diagonal matrices of the system parameters as follows; the time delay $h_j$ may be different for each service area

$$R = \operatorname{diag}\left[R_j\right]_{j=1}^k, B = \operatorname{diag}\left[B_j\right]_{j=1}^k, E$$

$$= \operatorname{diag}\left[e^{-sh_j}\right]_{j=1}^k,$$

$$G_p = \operatorname{diag}\left[G_{pj}\right]_{j=1}^k, G_tG_g = \operatorname{diag}\left[G_{tj}G_{gj}\right]_{j=1}^k,$$

$$X = \operatorname{diag}\left[X_j\right]_{j=1}^k, Y = I + XR^{-1}$$

$$P = XY^{-1} = Y^{-1}X \ \ \widehat{P} = \begin{bmatrix} PE & -Y^{-1}G_p \end{bmatrix}. \tag{30}$$

For any coprime factorization of the controller $C_j = D_j^{-1}N_j$, where $N_j, D_j \in \mathscr{H}_\infty$ and $D_j(\infty) \neq 0$, define

$$N = \operatorname{diag}\left[N_j\right]_{j=1}^k, \ \mathrm{D} = \operatorname{diag}\left[D_j\right]_{j=1}^k,$$

$$C = \operatorname{diag}\left[C_j\right]_{j=1}^k = \operatorname{diag}\left[D_j^{-1}N_j\right]_{j=1}^k = \mathrm{D}^{-1}\mathrm{N}. \tag{31}$$

The tie-line power flows among the $k$ interconnected areas are represented by the constant matrix $\Psi_T \in \mathbb{R}^{k \times k}$. Consider any right-coprime-factorization as

$$\frac{1}{s}\Psi_T = UV^{-1} \tag{32}$$

where $U, V \in \mathscr{H}_\infty^{k \times k}$, and $\det V(\infty) \neq 0$. The only closed right half-plane poles of $V^{-1}$ are at $s = 0$, although some entries do not have these poles since $\Psi_T$ is generally singular. The equations describing the closed-loop multiarea interconnected system $\mathscr{S}^k$ in Fig. 2 are as follows:

$$\begin{bmatrix} u \\ f \\ \xi \end{bmatrix} = \begin{bmatrix} I & 0 \\ 0 & V \\ 0 & \alpha U \end{bmatrix} \mathbf{D_H}^{-1} \begin{bmatrix} 0 & N \\ -Y^{-1}G_p & 0 \end{bmatrix} \begin{bmatrix} v \\ w \end{bmatrix} =: \mathbf{H} \begin{bmatrix} v \\ w \end{bmatrix},$$

$$\mathbf{D_H} := \begin{bmatrix} D & N(\alpha U + BV) \\ -PE & V + \alpha Y^{-1}G_pU \end{bmatrix}. \tag{33}$$

The multiarea interconnected system $\mathscr{S}^k$ is stable if the closed-loop map $\mathbf{H} \in \mathcal{M}(\mathscr{H}_\infty)$, equivalently, $\mathbf{D_H} \in \mathcal{M}(\mathscr{H}_\infty)$.

Theorem 1 states conditions for stability analysis of the multiarea interconnected system $\mathscr{S}^k$ under time delays based on a decentralized structure for the controllers $C_j$, where $j = 1, \ldots, k$. The method in Proposition 1 can be used to design each of the controllers $C_j$ of the $k$ subareas $j = 1, \ldots, k$. Since each area is individually stabilized, the analysis in Theorem 1 provides conditions for the stability of the interconnected system with the tie-line interconnections as well as the decentralized areas if the tie-line is broken.

**Theorem 1:** *Stability Analysis of Multiarea Systems With Time Delays.*

a) The multiarea interconnected system $\mathscr{S}^k$ is stable if and only if $\mathbf{W}^{-1} \in \mathcal{M}(\mathscr{H}_\infty)$, where $\mathbf{W}$ is given as

$$\mathbf{W} = [D + NEPB]V + \alpha[NEP + Y^{-1}G_pD]U$$

$$= D(V + \alpha Y^{-1}G_pU) + NEPB(V + \alpha B^{-1}U). \tag{34}$$

b) Let $C_j = D_j^{-1}N_j$ be a controller that stabilizes $P_j$ of area $j$ for each service area $j = 1, \ldots, k$. With the definitions in (31) and $M_j$ as given in (11), let $M := \operatorname{diag}\left[M_j\right]_{j=1}^k = (D + NEPB)$. Under these conditions, the multiarea interconnected system $\mathscr{S}^k$ is stable if and only if $\widetilde{\mathbf{W}}^{-1} \in \mathcal{M}(\mathscr{H}_\infty)$, where $\widetilde{\mathbf{W}}$ is given by

$$\widetilde{\mathbf{W}} = (I + \frac{\alpha}{s}(I + ECPB)^{-1}(ECP + Y^{-1}G_p)\Psi_T)V. \tag{35}$$

$\square$

*Proof of Theorem 1:*

a) The multiarea interconnected system $\mathscr{S}^k$ is stable if and only if $\mathbf{H} \in \mathcal{M}(\mathscr{H}_\infty)$ in the system description (33), which is equivalent to $\mathbf{D_H}^{-1} \in \mathcal{M}(\mathscr{H}_\infty)$. Since the diagonal matrices $N$, $D$, $P$, and $E$ commute, $\mathbf{H} \in \mathcal{M}(\mathscr{H}_\infty)$, these diagonal matrices commute, and $EPD^{-1}N =$

$D^{-1}EPN$ implies that $\mathbf{D_H}$ can be written as

$$\mathbf{D_H} = \begin{bmatrix} D & 0 \\ -PE & I \end{bmatrix} \begin{bmatrix} I & D^{-1}N(U+BV) \\ 0 & D^{-1}\mathbf{W} \end{bmatrix}. \quad (36)$$

By (36), $\det \mathbf{D_H} = \det \mathbf{W}$. Therefore, $\mathscr{S}^k$ is stable if and only if $\mathbf{W}^{-1} \in \mathcal{M}(\mathscr{H}_\infty)$ in (34).

b) Since $C_j$ is a stabilizing controller for $P_j$ for all $j$, it follows that $M^{-1} = (I + CPEB)^{-1}D^{-1} \in \mathcal{M}(\mathscr{H}_\infty)$. Rewrite (34) as $\mathbf{W} = M[V + \alpha M^{-1}(NEP + DY^{-1}G_p)U] = M\widetilde{\mathbf{W}}$. Since $M^{-1} \in \mathcal{M}(\mathscr{H}_\infty)$, the system $\mathscr{S}^k$ is stable if and only if $\widetilde{\mathbf{W}} \in \mathcal{M}(\mathscr{H}_\infty)$ in (35). $\qquad \square$

The controller $C_j$ stabilizes the $j$th service area if and only if $M_j^{-1} \in \mathscr{H}_\infty$, where $M_j$ is defined as in (11). For the interconnected system, the frequency deviation map $H^{fv}$ from $v$ to $f$ is $H^{fv} = -V\mathbf{W}^{-1}DY^{-1}G_p$. Therefore, if each of the controllers $C_j$ has integral action, then $D(0) = 0$ implies $H_j^{fv}(0) = 0$, and hence, the frequency deviation output $f_j$ due to constant load disturbance $v_j$ goes to zero asymptotically for each subarea of the interconnection under the tie-line interchange matrix $\Psi_T$. The stable controllers $\widetilde{C}_j$ in (12) or the special PD controller in (16) of Proposition 1-a) can also be designed for the individual service areas. However, with controllers that lack integral action, the frequency deviation would not approach zero in steady state.

Proposition 3 develops a decentralized controller design with integral action for the multiarea interconnected system $\mathscr{S}^k$ connected with a tie-line matrix $\Psi_T$. The design provides reliable stabilization in the sense that the stability of individual service areas is maintained, even when the tie-line is disconnected.

**Proposition 3:** *Integral Action Controller Design for Multi-area Systems With Time Delays.* If $(V + Y^{-1}G_pU)^{-1} \in \mathcal{S}^{k \times k}$, then let $\alpha = 1$. Otherwise, let $\alpha \in \mathbb{R}_+$ be such that $(V + \alpha Y^{-1}G_pU)^{-1} \in \mathcal{S}^{k \times k}$. Define $\Theta$, $L_1$, $L_2$, and $L_3 \in \mathcal{S}^{k \times k}$ as

$$\Theta := (I + \frac{\alpha}{s}B^{-1}\Psi_T)(I + \frac{\alpha}{s}Y^{-1}G_p\Psi_T)^{-1} \quad (37)$$

$$L_1 := \mathrm{diag}\left[h_j\tilde{\beta}_j(1+sQ_j)P_j\right]_{j=1}^k \Theta \quad (38)$$

$$L_2 := s^{-1}\left[\mathrm{diag}\left[(1+sQ_j)P_j\right]_{j=1}^k \Theta - \Theta_o\right] \quad (39)$$

$$L_3 := s^{-1}\left[\mathrm{diag}\left[\tilde{\beta}_j\rho_j - \tilde{\beta}_j(1+sQ_j)P_j\right]_{j=1}^k\right] \quad (40)$$

where $\Theta_o = \mathrm{diag}\left[\rho_j\right]_{j=1}^k \Theta(0)$.

a) The integral action controller $C = \mathrm{diag}\left[C_j\right]_{j=1}^k$ is designed such that $C_j$ in the $j$th service area is

$$C_j = \frac{\beta\tilde{\beta}_j(1+sQ_j)}{B_j[(s+\beta\tilde{\beta}_j\rho_j) - \beta\tilde{\beta}_j(1+sQ_j)P_j]} \quad (41)$$

where $\tilde{\beta}_j \in \mathbb{R}_+$ and $\beta \in (0,1]$ satisfy the following:

$$\tilde{\beta}_j < \frac{1}{h_j\|(1+sQ_j)P_j\|} \quad (42)$$

$$\beta < \frac{1}{\|L_1\| + \|L_2 + L_3\|}. \quad (43)$$

b) *Special Case (PID Controllers):* For any $K_{pj}, K_{dj} \in \mathbb{R}$, and $\tau_j \in \mathbb{R}_+$, let $\tilde{\beta}_j \in \mathbb{R}_+$ satisfy the norm condition (19) as follows:

$$\tilde{\beta}_j < [\|(K_{pj} + \frac{K_{dj}s}{\tau_j s + 1})P_j + \frac{P_j - \rho_j}{s}\|$$
$$+ h_j\|(K_{pj}s + \frac{K_{dj}s^2}{\tau_j s + 1} + 1)P_j\|]^{-1}. \quad (44)$$

Define $L_1$, $L_2$, and $L_3$ as (38)–(40) with $Q_j$ defined as in (26), i.e.,

$$Q_j = (K_{pj} + \frac{K_{dj}s}{\tau_j s + 1})[1 + \beta_j(K_{pj} + \frac{K_{dj}s}{\tau_j s + 1})P_j]^{-1}. \quad (45)$$

Let $\beta \in \mathbb{R}_+$ satisfy (43). Then, a special case of the controller in (41) is a PID controller as

$$C_{\mathrm{pid}} = \frac{\beta\tilde{\beta}_j}{B_j}\left[K_{pj} + \frac{K_{dj}s}{\tau_j s + 1} + \frac{1}{s}\right]. \quad (46)$$

$\qquad \square$

**Remarks 2:**

a) The design procedure in Proposition 3 requires $(V + \alpha Y^{-1}G_pU)$ to be unimodular, i.e., $(V + \alpha Y^{-1}G_pU)^{-1} \in \mathcal{S}^{k \times k}$. For the given tie-line matrix coefficients, $(V + \alpha Y^{-1}G_pU)$ is generally unimodular for $\alpha = 1$. It should be noted that $(V + \alpha Y^{-1}G_pU)$ depends on the system parameters $Y^{-1}G_p$ and on the tie-line matrix $s^{-1}\Psi = UV^{-1}$, but it does not depend on the designed controllers. In the special case of two service areas discussed in Remark 2-b), a sufficient condition is given in (49) for choosing $\alpha \in \mathbb{R}_+$ to make $(V + \alpha Y^{-1}G_pU)$ unimodular.

b) *Special Case: Controller Design for a Two-Area System With Time Delays.* The multiarea controller design in Proposition 3 is simplified for the special case of two-area interconnected systems. For $k = 2$, the interaction through the tie-line is given as $\phi_j = \frac{\alpha}{s}\psi_j(f_1 - f_2)$, where $\psi_j \geq 0$ for $j = 1, 2$. The tie-line matrix is

$$\Psi_T = \begin{bmatrix} \psi_1 & -\psi_1 \\ -\psi_2 & \psi_2 \end{bmatrix}. \quad (47)$$

For any $a \in \mathbb{R}_+$, a right-coprime-factorization of $(\frac{1}{s}\Psi_T) = UV^{-1}$ as in (32) is

$$\frac{1}{s}\Psi_T = UV^{-1} = \frac{1}{(s+a)}\begin{bmatrix} \psi_1 & 0 \\ -\psi_2 & 0 \end{bmatrix}\begin{bmatrix} \frac{s}{(s+a)} & 1 \\ 0 & 1 \end{bmatrix}^{-1}. \quad (48)$$

A sufficient condition for $\Theta \in \mathcal{M}(\mathcal{S})$, equivalently, $(V + \alpha Y^{-1} G_p U)$ unimodular, is to choose any $\alpha \in \mathbb{R}_+$ satisfying the following:

$$\alpha < \|s^{-1}\left[\sum_{j=1}^{2} \psi_j (Y_j^{-1} G_{pj} - \rho_j)\right]\|^{-1}. \qquad (49)$$

The controllers $C_1$ and $C_2$ are designed as (41) in Proposition 3, where $\tilde{\beta}_j > 0$ satisfies (42), and $\beta \in (0, 1]$ satisfies (43), where $\Theta$ in (37) becomes

$$\Theta = (1 + \frac{\alpha}{s} \sum_{j=1}^{2} \psi_j Y_j^{-1} G_{pj})^{-1} \widetilde{W} \qquad (50)$$

where

$$\widetilde{W} = I + \frac{\alpha}{s}$$
$$\begin{bmatrix} (\psi_2 Y_2^{-1} G_{p2} + \psi_1 B_1^{-1}) & \psi_1 (Y_1^{-1} G_{p1} - B_1^{-1}) \\ \psi_2 (Y_2^{-1} G_{p2} - B_2^{-1}) & (\psi_1 Y_1^{-1} G_{p1} + \psi_2 B_2^{-1}) \end{bmatrix}.$$

c) The norm condition (42) in Proposition 3-a) and the norm condition (44) in Proposition 2-b) determine a conservative bound on the controller parameter $\tilde{\beta}_j$ for fixed time delays $h_j$ in each of the service areas. As in the case of individual service areas explained in Remark 1, the value of $h_j$ used for these norm computations can be regarded as guaranteed upper bounds on the time delays, but the designed controllers robustly stabilize the multiarea system for any time delays smaller than $h_j$ as well. Due to the conservatism in the small-gain condition, the designed decentralized controllers may actually result in delay margins larger than the prespecified $h_j$ values for each service area. $\qquad \square$

*Proof of Proposition 3:* Let $\beta_j = \beta \tilde{\beta}_j$. With $C_j$ as in (41), the controller is $C = D^{-1} N$, where

$$D = (sI + \Theta_o)^{-1} \mathrm{diag}\left[(s + \beta_j \rho_j) - \beta_j (1 + s Q_j) P_j\right]_{j=1}^{k}$$

$$N = \beta (sI + \Theta_o)^{-1} \mathrm{diag}\left[\tilde{\beta}_j (1 + s Q_j) B_j^{-1}\right]_{j=1}^{k}. \qquad (51)$$

Since $\beta \leq 1$ implies $\beta_j = \beta \tilde{\beta}_j$ and satisfy (15), by Proposition 1-b), each $C_j$ stabilizes the $j$th service area. By Theorem 1, with $D$ and $N$ as in (51), the interconnected system $\mathscr{S}^k$ is stable if and only if $\mathbf{W} \in \mathcal{M}(\mathscr{H}_\infty)$ is unimodular. With $(V + \alpha Y^{-1} G_p U)^{-1} \in \mathcal{M}(\mathcal{S})$ implying $\Theta = (V + \alpha B^{-1} U)(V + \alpha Y^{-1} G_p U)^{-1} \in \mathcal{M}(\mathcal{S})$, the system is stable if and only if $\mathbf{W}(V + \alpha Y^{-1} G_p U)^{-1}$ is unimodular, where

$$\mathbf{W}(V + \alpha Y^{-1} G_p U)^{-1} = D + NEPB\Theta$$

$$= (sI + \Theta_o)^{-1} \mathrm{diag}\left[(s + \beta_j \rho_j) - \beta_j (1 + s Q_j) P_j\right]_{j=1}^{k}$$

$$+ (sI + \Theta_o)^{-1} \mathrm{diag}\left[\beta_j (1 + s Q_j)\right]_{j=1}^{k} EP\Theta$$

$$= I + \beta s (sI + \Theta_o)^{-1} \left[\mathrm{diag}\left[\frac{(e^{-sh_j} - 1)}{h_j s}\right]_{j=1}^{k} L_1 + L_2 + L_3\right]. \qquad (52)$$

Using the norm equalities $\|(h_j s)^{-1}(e^{-sh_j} - 1)\| = 1$ and $\|s(sI + \Theta_o)^{-1}\| = 1$, for $\beta$ satisfying (43), it follows that

$$\beta \|s(sI + \Theta_o)^{-1} \left[\left[\frac{(e^{-h_j s} - 1)}{h_j s}\right]_{j=1}^{k} L_1 + L_2 + L_3\right]\|$$
$$\leq \beta(\|L_1\| + \|L_2 + L_3\|) < 1. \qquad (53)$$

Therefore, $\mathbf{W} \in \mathcal{M}(\mathscr{H}_\infty)$ is unimodular, and hence, the proposed decentralized controller structure stabilizes the interconnected system. $\qquad \square$

## III. NUMERICAL STUDIES

Consider a multiarea interconnected system with two service areas, with a nonreheated turbine as in (3) in service area 1, and a reheated turbine as in (4) in service area 2. The plant parameters are typical values as in, e.g., [5], [6], [12], [13], and [20].

Let the plant as in (8) in service area 1 have a nonreheated turbine as in (3), where the load, governor, turbine, and droop model parameters in (1) and (3) are given as

$$K_1 = 120, \; T_{p1} = 20, \; T_{g1} = 0.3, \; T_{t1} = 0.08, \; R_1 = 2.4$$

$$X_1(s) = \frac{120}{(20s + 1)(0.3s + 1)(0.08s + 1)}$$

$$P_1(s) = \frac{120}{0.48s^3 + 7.624s^2 + 20.38s + 51}. \qquad (54)$$

Service area 2 has a reheated turbine as (4), with the parameters of service area 1, and $T_{r2} = 4.2$ and $c_{r2} = 0.35$. From (6), we have

$$X_2(s) = \frac{120(1.47s + 1)}{(20s + 1)(0.3s + 1)(0.08s + 1)(4.2s + 1)},$$

$$P_2(s) = \frac{120(1.47s + 1)}{2.016s^4 + 32.5008s^3 + 93.22s^2 + 98.08s + 51}. \qquad (55)$$

Then, $\rho_1 = \rho_2 = \rho = 120/51$. Let the frequency bias factors be $B_1 = B_2 = 0.425$. Let the two-area system be connected through a tie-line as shown in Fig. 2, where the tie-line matrix is given by (47), with $\psi_1 = \psi_2 = 0.545$. For these tie-line gains, $(V + Y^{-1} G_p U)$ is unimodular. Therefore, $\alpha = 1$ works; but a more conservative choice for $\alpha \in \mathbb{R}_+$ is obtained from the sufficient condition (49), which is satisfied for $\alpha < 0.2856$. In the controller design, we choose $\alpha = 0.285$ in the definition of $\Theta$.

a) Following Proposition 3-a), $C_1$ and $C_2$ are designed as in (41). The parameters $Q_1$ and $Q_2$ can be chosen to satisfy various design specifications. In this design, there are no requirements other than closed-loop stability in the presence of time delays and zero frequency deviation outputs in steady state due to constant load disturbances. Other values for $Q_j$ can be explored to satisfy additional constraints and possibly for larger delay margins. For $Q_1 = 0$, (42) holds for $\tilde{\beta}_1 < 0.3508 h_1^{-1}$. Similarly, for $Q_2 = 0$, (42) holds for $\tilde{\beta}_2 < 0.3351 h_2^{-1}$. With $Q_j = 0$, (38)–(40) can be written as follows: $L_1 = \mathrm{diag}\left[h_j \tilde{\beta}_j P_j\right]_{j=1}^{k} \Theta$, $L_2 = s^{-1}[\mathrm{diag}\left[P_j\right]_{j=1}^{k} \Theta -$
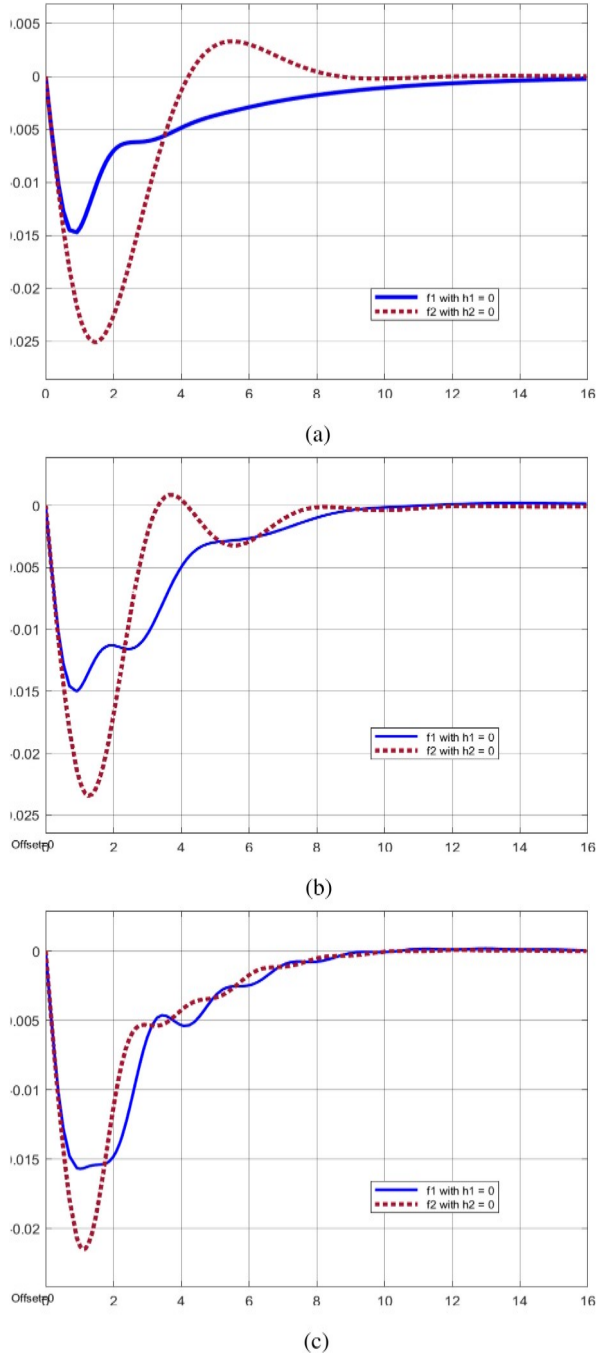
Fig. 3. Frequency deviation outputs $f_1$ and $f_2$ with load disturbances $v_1 = v_2 = 0.01$, with no time delays $h_1 = h_2 = 0$.



Fig. 4. Frequency deviation outputs $f_1$ and $f_2$ with load disturbances $v_1 = v_2 = 0.01$, with time delays of $h_1 = h_2 = 2$ s.

$\Theta_o]$, and $L_3 = s^{-1}\text{diag}\left[\tilde{\beta}_j \rho_j - \tilde{\beta}_j P_j\right]_{j=1}^{k}$, where $\Theta_o = \rho I_2$. For $h_1 = h_2 = 2$ s and $\tilde{\beta}_1 = \tilde{\beta}_2 = 0.33 h_1^{-1}$, the norms are computed as $\|L_1\| = 1.0949$, $\|L_2 + L_3\| = 0.4669$. Then, (43) is satisfied for $\beta < 0.6403$. Using $\beta = 0.64$, the integral action controllers $C_1 = N_{c1}/D_{c1}$ and $C_2 = N_{c2}/D_{c2}$, as given in (41), are

$$N_{c1} = 0.2485(0.48s^3 + 7.624s^2 + 20.38s + 51)$$

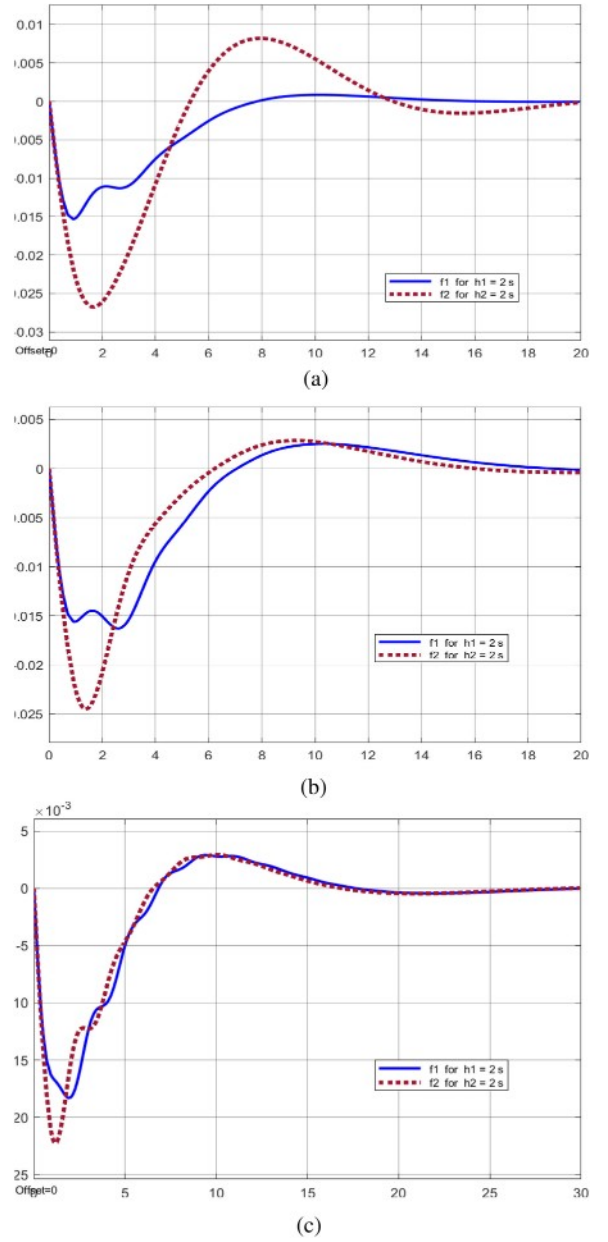$$D_{c1} = s(0.4800s^3 + 7.7433s^2 + 22.2743s + 56.0638)$$

$$N_{c2} = 0.2485(2.016s^4 + 32.5008s^3 + 93.22s^2$$
$$+ 98.08s + 51)$$

$$D_{c2} = s(2.0160s^4 + 33.0017s^3 + 101.2955s^2$$
$$+ 121.2424s + 56.7422). \tag{56}$$

Applying load disturbances $v_1 = v_2 = 0.01$ in each of the service areas, the frequency deviation outputs $f_1$ and $f_2$ are plotted in Fig. 3 for the case of no time delay in the service areas. Fig. 3(a) shows the frequency deviation outputs of each service area with disconnected interconnection tie-line between the channels, where each controller $C_j$ stabilizes the $j$th service area. Fig. 3(b) shows the frequency deviation outputs with $\alpha = 0.285$ satisfying the sufficient condition (49) to make the interconnection
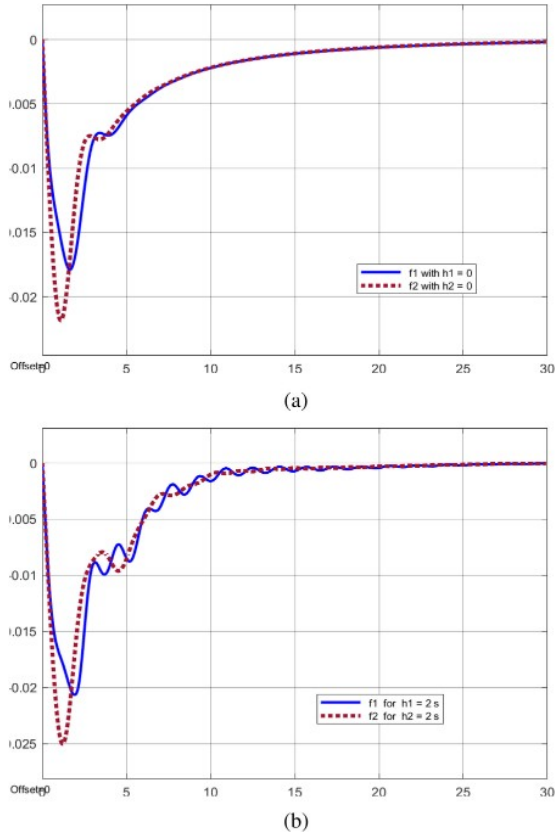
**Fig. 5.** Frequency deviation outputs $f_1$ and $f_2$ with load disturbances $v_1 = v_2 = 0.01$, with no time delays and with time delays of $h_1 = h_2 = 2$ s using PID controllers.

stable with the tie-line. Fig. 3(c) shows the frequency deviation outputs with $\alpha = 1$, since $(V + Y^{-1}G_pU)$ is unimodular. Due to the integral action in the controllers, the steady-state frequency deviations are zero for each channel with any amount of delay as expected.

Fig. 4 repeats the plots of Fig. 3 but with delays of $h_1 = h_2 = 2$ s in each channel. Fig. 4(a) shows the frequency deviation outputs $f_1$ and $f_2$ of each service area with load disturbances $v_1 = v_2 = 0.01$, where the interconnection tie-line between the channels is disconnected. Fig. 4(b) shows the frequency deviation outputs with $\alpha = 0.285$ satisfying the sufficient condition (49) to make the interconnection stable with the tie-line. Fig. 4(c) shows the frequency deviation outputs with $\alpha = 1$ since $(V + Y^{-1}G_pU)$ is unimodular. Due to the integral action in the controllers, the steady-state frequency deviations are zero for each case as expected. b) The integral action controllers $C_1$ and $C_2$ designed with parameters as in (56) are fourth- and fifth-order controllers. Now, for the same service areas defined by $P_1$ in (54) and $P_2$ in (55), following Proposition 3, we design the alternate PID controllers given in (46). Choosing $K_{p1} = 0.2$, $K_{d1} = 0.8$, $K_{p2} = 0.4$, $K_{d2} = 1$, and $\tau_1 = \tau_2 = 0.005$, conditions (19) and (43) are satisfied by choosing $\beta\tilde{\beta}_1/B_1 = 0.2$ and $\beta\tilde{\beta}_2/B_2 = 0.1$. The PID controllers are

$$C_1 = \frac{0.1602s^2 + 0.041s + 0.2}{s(0.005s + 1)} \tag{57}$$

$$C_2 = \frac{0.1002s^2 + 0.0405s + 0.1}{s(0.005s + 1)}. \tag{58}$$

With these PID controllers, applying load disturbances $v_1 = v_2 = 0.01$ in each of the service areas, the frequency deviation outputs $f_1$ and $f_2$ are plotted in Fig. 5. The case of no time delay in the service areas is shown in Fig. 5(a), and Fig. 5(b) shows the frequency deviation with delays of 2 s in each service area. In both cases, the tie-line is connected with $\alpha = 1$. Due to the integral action in the controllers, the steady-state frequency deviations are zero for each channel with any amount of delay as expected.

A comparison of the frequency deviation outputs shown in Fig. 5 with the previous simulation results shown in Figs. 3 and 4 shows that the PID controller with the chosen parameters results in a longer settling time than the higher order controllers $C_1$ and $C_2$ with the chosen parameters and $Q_1 = Q_2 = 0$. On the other hand, the PID design does not have any significant overshoot even for the case of 2-s delays in each service area. If specific time-domain constraints are given in the design requirements, then different values of $Q_1$ and $Q_2$ can be explored to satisfy those constraints.

## IV. CONCLUSION

A simple and systematic decentralized controller design procedure was developed for closed-loop stability and integral action large scale multiarea power system interconnections subject to time delays. Proposition 1 developed a general controller parameterization for individual service areas, where the parameters $Q_j \in \mathcal{S}$ can be chosen to satisfy additional design specifications. The parameter selections allowed low-order controller implementation, which was treated in Proposition 2 for the special cases of PD and PID controllers. The controller gains can be adjusted to ensure robust stability and steady-state accuracy for all expected time delays. Then, the decentralized controller design for the individual subsystems was modified in Proposition 3-a) so that closed-loop stability and integral action were maintained when the service areas were interconnected via a tie-line in a large scale multiarea configuration. The proposed design was based on the necessary and sufficient stability conditions stated in Theorem 1, where the individual service areas interacted due to the tie-line connection, and each subsystem may be subject to different time delays. Similar to the case of individual service areas, Proposition 3-b) specialized the multiarea design to PID controllers. The frequency deviation outputs due to constant load disturbances in all service areas go to zero due to the integral action in the designed controllers. The customization of controller parameters for specific applications and additional performance objectives can be explored further.

## REFERENCES

[1] P. Kundur *et al.*, "Definition and classification of power system stability," *IEEE Trans. Power Syst.*, vol. 19, no. 3, pp. 1387–1401, Aug. 2004.
[2] T. C. Yang, Z. T. Ding, and H. Yu, "Decentralised power system load-frequency control beyond the limit of diagonal dominance," *Int. J. Elect. Power Energy Syst.*, vol. 24, pp. 173–184, 2002.
[3] H. Bevrani, *Robust Power System Frequency Control*. Boston, MA, USA: Springer, 2009.

[4] H. Bevrani, M. Watanabe, and Y. Mitani, *Power System Monitoring and Control*. Hoboken, NJ, USA: Wiley, 2014.

[5] W. Tan, "Tuning of PID load frequency controller for power systems," *Energy Convers. Manage.*, vol. 50, no. 6, pp. 1465–1472, 2009.

[6] W. Tan, "Unified tuning of PID load frequency controller for power systems via IMC," *IEEE Trans. Power Syst.*, vol. 25, no. 1, pp. 341–350, Feb. 2010.

[7] M. N. Anwar and S. Pan, "A new PID load frequency controller design method in frequency domain through direct synthesis approach," *Elect. Power Energy Syst.*, vol. 67, pp. 560–569, 2015.

[8] G. Shahgholian, S. Yazdekhasti, and P. Shafaghi, "Dynamic analysis and stability of the load frequency control in two area power system with steam turbine," in *Proc. Int. Conf. Comput. Elect. Eng.*, 2009, pp. 30–34.

[9] G. Ray, A. N. Prasad, and G. D. Prasad, "A new approach to the design of robust load frequency controller for large scale power systems," *Elect. Power Syst. Res.*, vol. 51, pp. 13–22, 1999.

[10] L. Dong and Y. Zhang, "On design of a robust load frequency controller for interconnected power systems," in *Proc. Amer. Control Conf.*, 2010, pp. 1731–1736.

[11] L. Dong, "Decentralized load frequency control for an interconnected power system with nonlinearities," in *Proc. Amer. Control Conf.*, 2016, pp. 5915–5920.

[12] X. F. Yu and K. Tomsovic, "Application of linear matrix inequalities for load frequency control with communication delays," *IEEE Trans. Power Syst.*, vol. 19, no. 3, pp. 1508–1519, Aug. 2004.

[13] A. N. Gündeş and L. Chow, "Controller synthesis for single-area and multi-area power systems with communication delays," in *Proc. Amer. Control Conf.*, 2013, pp. 970–975.

[14] A. N. Gündeş and L. C. Chow, "Controllers for interconnected systems with communication delays," in *Proc. 54th IEEE Conf. Decis. Control*, 2015, pp. 7084–7089.

[15] L. Jiang, W. Yao, Q. H. Wu, J. Y. Wen, and S. J. Cheng, "Delay-dependent stability for load frequency control with constant and time-varying delays," *IEEE Trans. Power Syst.*, vol. 27, no. 2, pp. 932–941, May 2012.

[16] C.-K. Zhang, L. Jiang, Q. H. Wu, Y. He, and M. Wu, "Delay-dependent robust load frequency control for time delay power systems," *IEEE Trans. Power Syst.*, vol. 28, no. 3, pp. 2192–2201, Aug. 2013.

[17] H. Bevrani and T. Hiyama "Robust decentralised PI based LFC design for time delay power systems," *Energy Convers. Manage.*, vol. 49, no. 2, pp. 193–204, 2008.

[18] X.-C. Shangguan *et al.*, "Robust load frequency control for power system considering transmission delay and sampling period," *IEEE Trans. Ind. Informat.*, vol. 17, no. 8, pp. 5292–5303, Aug. 2021.

[19] X.-C. Shangguan *et al.*, "Switching system-based load frequency control for multi-area power system resilient to denial-of-service attacks," *Control Eng. Pract.*, vol. 107, 2021, Art. no. 104678.

[20] P. Kundur, N. J. Balu, and M. G. Lauby, *Power System Stability and Control*. New York, NY, USA: McGraw-Hill, 1994.

**A. N. Gündeş** received the B.S., M.S., and Ph.D. degrees in electrical engineering and computer science from the University of California at Berkeley, Berkeley, CA, USA, in 1988.

She is currently a Professor of electrical and computer engineering with the University of California, Davis, CA, USA.

**L. A. Kabuli** received the B.S. degree in electrical engineering and computer sciences and the B.A. degee in music in 2021 from the University of California at Berkeley, Berkeley, CA, USA, where she is currently working toward the Ph.D. degree in electrical engineering and computer sciences.